Physics of Wave Processes and Radio Systems
2023, vol. 26, no. 1, pp. 93–105

DOI 10.18469/1810-3189.2023.26.1.93-105

Received 6 December 2022
Accepted 9 January 2023

Investigation of the electromagnetic properties of a transverse insert based on a planar layer of a chiral metamaterial in a rectangular waveguide

Ivan Yu. Buchnev, Oleg V. Osipov

Povolzhskiy State University of Telecommunications and Informatics
23, L. Tolstoy Street,
Samara, 443010, Russia

Abstract – The paper considers the solution of the problem of diffraction of the fundamental wave of a rectangular waveguide H_{10} on a planar transverse insert based on a chiral metamaterial created on the thin-wire conducting helices. To describe the chiral layer, a particular mathematical model is constructed that takes into account the properties of heterogeneity and dispersion of the permittivity and the chirality parameter of the artificial media. The well-known in physics model of Maxwell Garnett was used to take into account the heterogeneity property. To take into account the permittivity dispersion the Drude–Lorentz formula was applied and for the chirality parameter was used the Condon formula. The problem of diffraction of the rectangular waveguide main wave on a planar layer of a chiral metamaterial was solved by the partial regions method and was reduced to a system of linear algebraic equations for unknown reflection and transmission coefficients. It is shown that in the presence of a transverse chiral layer in the waveguide structure, a wave of the H_{01} type cross-polarized with respect to the main one arises. An analysis of the frequency dependences of the moduli of the reflection and transmission coefficients of the fundamental H_{10} and cross-polarized H_{01} showed that in some narrow frequency intervals in the single-mode gap, situations arise when the fundamental wave type is replaced from H_{10} to H_{01} near resonant frequencies. The transmission line under consideration can find application in the creation of frequency selective filters and polarization converters in the microwave range.

Keywords – chiral media; chiral metamaterial; metamaterial; helix; spatial dispersion; frequency selectivity; Maxwell Garnett model; Condon model; rectangular waveguide; single-mode; fundamental mode; cross-polarization.

Introduction

The electromagnetic properties of various artificial structures, known as metamaterials are currently under active study [1–5]. This is due to the fact that the use of composite media allows for the achievement of new electromagnetic properties that are unattainable with traditional materials. A metamaterial is a spatial composition of a medium, acting as a container, within which areas or volumes are replaced with a material of a different type. For the microwave range, the containers are usually dielectric and the embedded areas are conductive. At the development stage, it is possible to design the metamaterial structure to achieve the desired properties of electromagnetic field interaction. In most cases, resonant conductive microelements serve as the implanted areas. When these microelements have a mirror-like asymmetric shape, the metamaterial is usually referred to as chiral (from the Greek χιρο – "hand") [6–10]. In the classical sense, a chiral metamaterial is a composite medium consisting of a dielectric container in which uniformly placed and randomly oriented conductive microelements of mirror asymmetric shape are embedded. Several different types of chiral elements have been considered in the scientific literature, namely three-dimensional (such as Tellegen elements, single- and multiturn spirals, and mutually orthogonal spirals) and two-dimensional (such as S-elements, gammadions, open rings, and Archimedes spirals). Chiral materials are characterized by the propagation of two waves with right- and left-handed circular polarizations, as well as the cross-polarization of the field. These chiral metamaterials (CMM) are currently being actively used in microwave and antenna technologies. Their main include circulators, phase shifters, filters, antennas on CMM substrates, and chiral transmission lines, among others. [11–13]. It is important to note here that because chiral microelements are resonant particles, microwave devices based on CMM will exhibit frequency-selective properties.

The use of CMMs within microwave transmission line structures has garnered significant interest. Initial research on this topic was published in 1988 [14]. This study investigated the natural waves of a plane chiral waveguide bounded by ideally conducting planes. Further detailed studies have since been conducted on wave propagation in both open and closed circular uniformly filled chiral waveguides [15–17]. In [18], the natural waves of a plane two-layer chiral dielectric waveguide were studied, without restrictions on the structure thickness. A detailed theory of natural wave propagation in microwave guides is

✉ o.osipov@psuti.ru (*Oleg V. Osipov*)

CC BY © Buchnev I.Yu., Osipov O.V., 2023

presented in [19]. Additionally, waves in chiral waveguides with impedance walls have been analyzed [20]. The analysis of rectangular cross-section waveguides requires the use of numerical methods [21]. In [22], an analysis of the natural waves of a planar chiral waveguide was performed. Technologies for creating chiral and bi-anisotropic waveguides are discussed in [23].

Interestingly, most of the aforementioned studies employ a standard mathematical model of a chiral medium, based on the Lindell–Sivola formalism [6]. This model uses material equations in the harmonic signal mode with vectors dependent on time in form $\exp(i\omega t)$):

$$\vec{\mathbf{D}} = \varepsilon\vec{\mathbf{E}} \mp i\chi\vec{\mathbf{H}}, \quad \vec{\mathbf{B}} = \mu\vec{\mathbf{H}} \pm i\chi\vec{\mathbf{E}}, \tag{1}$$

where $\vec{\mathbf{E}}$, $\vec{\mathbf{H}}$, $\vec{\mathbf{D}}$, $\vec{\mathbf{B}}$ are the complex amplitudes of the vectors of intensity and induction of electric and magnetic fields, i is an imaginary unit; ε is the relative dielectric permeability of the CMM; μ is the relative magnetic permeability of the CMM; χ is the relative chirality parameter. In Eq. (1), the upper signs correspond to the CMM based on mirror asymmetric microelements with a right twist, while the lower signs correspond to the CMM based on mirror asymmetric microelements with a left twist. The relationships of Eq. (1) are presented in the Gaussian system of units.

It is worth noting that most research assumes that the material parameters are constant, unaffected by the frequency of the incident electromagnetic field, and that the CMM is homogeneous. In other words, these studies do not consider the difference in the parameter values for the container and regions occupied by chiral microelements when calculating the effective dielectric permeability.

However, some studies have proposed generalized and specific mathematical models of chiral metamaterials that do not consider dispersion and heterogeneity [24–26]. Heterogeneity arises owing to the CMM composition: a container environment combined with areas possessing different material parameters, where mirror-like asymmetric microelements are located.

Some mathematical models of CMM are described in [34; 35].

In this study, we present a unique mathematical model for a metamaterial that factors in chirality, dispersion, and heterogeneity to accurately depict the electromagnetic properties of the chiral layer. This metamaterial is created based on a uniform assembly of thin-wire conductive spiral elements.

The primary objective of this research was to address the diffraction problem of the fundamental wave of a rectangular waveguide H_{10} on a transverse insert made of CMM. In this case, a model featuring frequency-dependent parameters $\varepsilon(\omega)$; $\chi(\omega)$ is employed to describe the chiral layer.

1. Development of a private mathematical model of CMM based on thin-wire spiral microelements

Let us delve into the structure of a metamaterial consisting of a dielectric container with relative dielectric and magnetic permeabilities ε_c, μ_c, where mirror-like asymmetric conductive microelements are placed. The regions inhabited by these mirror-like asymmetric elements possess relative dielectric and magnetic permeabilities ε_s, μ_s. The linear dimensions of these regions are denoted by d and l represents the distance between adjacent elements. A general block diagram of the CMM is presented in Fig. 1.

The effective dielectric and magnetic permeabilities of the metamaterial functionally depend on the permeabilities of both the container and chiral regions, namely $\varepsilon = \varepsilon(\varepsilon_c, \varepsilon_s)$; $\mu = \mu(\mu_c, \mu_s)$.

These functional dependencies for heterogeneous media are determined by various models, such as the Maxwell Garnett model and the Bruggeman model, among others [27–29].

The Maxwell Garnett model uses the following functional relationships:

$$\varepsilon = \varepsilon_c \frac{1+2\alpha\varepsilon_x}{1-\alpha\varepsilon_x}; \quad \varepsilon_x = \frac{\varepsilon_s - \varepsilon_c}{\varepsilon_s + 2\varepsilon_c}, \tag{2}$$

where ε represents the relative effective dielectric permeability of the metamaterial; ε_c stands for the relative dielectric permeability of the container; ε_s indicates the relative dielectric permeability of chiral regions; and α is volume concentration of the chiral regions.

To accommodate the dispersion of dielectric permeability of chiral regions, we use the Drude–Lorentz equation:

$$\varepsilon_s(\omega) = \varepsilon_\infty + \frac{(\varepsilon_c - \varepsilon_\infty)\omega_p^2}{\omega_0^2 + 2i\delta_e\omega - \omega^2}, \tag{3}$$

where ε_∞ is the asymptotic value of the dielectric permeability at $\omega \to \infty$; δ_e is the damping coefficient; ω_p^2 represents resonant frequency of absorption; and ω_0^2 is the resonant frequency of the microelement,

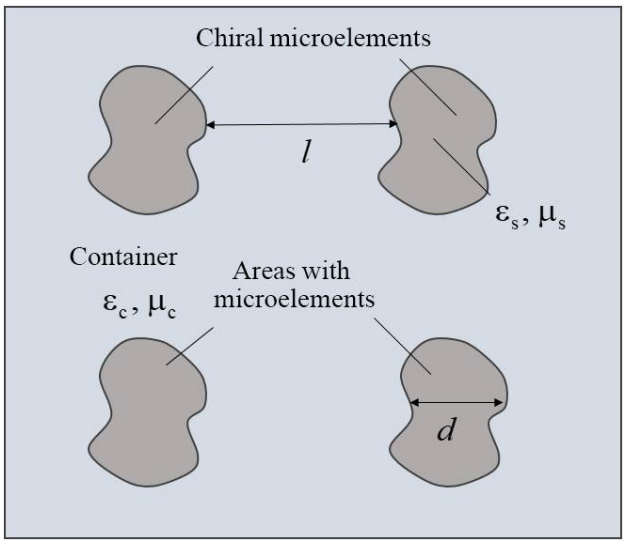

Fig. 1. Structural general scheme of the metamaterial
Рис. 1. Структурная общая схема метаматериала

which is then calculated for a specific chiral microelement in a quasistationary approximation.

To consider the dispersion of the chirality parameter, we use the Condon equation [30–31]:

$$\chi(\omega) = \frac{\omega_0^2 \beta_0 \omega}{\omega_0^2 + 2i\delta_x \omega_0 \omega - \omega^2}, \quad (4)$$

where β_0 is a constant with an inverse time dimension and describes the degree of mirror asymmetry of the microelement; and δ_x is the damping coefficient of the chirality parameter.

Considering Eqs. (2) and (3), we obtain the following equation for the frequency-dependent effective dielectric permeability of the CMM:

$$\varepsilon(\omega) = \varepsilon_c \frac{1 + 2\alpha\varepsilon_x(\omega)}{1 - \alpha\varepsilon_x(\omega)}; \quad (5)$$

$$\varepsilon_x = \frac{\varepsilon_\infty + \dfrac{(\varepsilon_c - \varepsilon_\infty)\omega_p^2}{\omega_0^2 + 2i\delta_e\omega - \omega^2} - \varepsilon_c}{\varepsilon_\infty + \dfrac{(\varepsilon_c - \varepsilon_\infty)\omega_p^2}{\omega_0^2 + 2i\delta_e\omega - \omega^2} + 2\varepsilon_c},$$

The material equations for a chiral metamaterial (without considering the type of microelement) considering Eqs. (1), (4), and (5) have the following form:

$$\vec{\mathbf{D}} = \varepsilon(\omega)\vec{\mathbf{E}} \mp i\chi(\omega)\vec{\mathbf{H}}, \quad \vec{\mathbf{B}} = \mu\vec{\mathbf{H}} \pm i\chi(\omega)\vec{\mathbf{E}}; \quad (6)$$

$$\varepsilon(\omega) = \varepsilon_c \frac{1 + 2\alpha\varepsilon_x(\omega)}{1 - \alpha\varepsilon_x(\omega)}; \quad \chi(\omega) = \frac{\omega_0^2 \beta_0 \omega}{\omega_0^2 + 2i\delta_x\omega_0\omega - \omega^2};$$

$$\varepsilon_x = \frac{\varepsilon_s(\omega) - \varepsilon_c}{\varepsilon_s(\omega) + 2\varepsilon_c}; \quad \varepsilon_s(\omega) = \varepsilon_\infty + \frac{(\varepsilon_c - \varepsilon_\infty)\omega_p^2}{\omega_0^2 + 2i\delta_e\omega - \omega^2}.$$

The mathematical model of Eq. (6) is applicable when all chiral microelements have identical shapes and linear dimensions, are equidistantly located, chaotically oriented, and the magnetic permeability of the CMM remains frequency-independent.

Based on Eq. (6), we construct a particular mathematical model for the CMM based on a specific type of a mirror asymmetric element.

Next, we consider the calculation of the resonant frequency of a thin-wire conducting element in a quasistationary approximation [32].

The structure of a CMM cell based on a thin-wire spiral element is shown in Fig. 2. Figure 3 presents a cross-section of a spiral microelement.

In Fig. 3, the following designations are introduced: *H* is the container height; *d* is the distance between the spiral turns; *R* is the internal radius of the spiral; *r* is the wire radius; α refers to the spiral winding angle; and *N* indicates the number of spiral turns.

To calculate the resonant frequency in a quasistatic approximation, we use Thomson's equation :

$$\omega_0 = \frac{1}{\sqrt{LC}}, \quad (5)$$

where *L* is the inductance of the spiral; and *C* is the spiral capacity.

The inductance of the spiral is calculated by the following equation:

$$L = \mu_c \frac{N^2 S}{g} = \mu_c \frac{\pi N^2 R^2}{g}, \quad (6)$$

where *S* is the area of the spiral turn; *g* is the length of the unrolled wire; and *R* is the internal radius of the spiral.

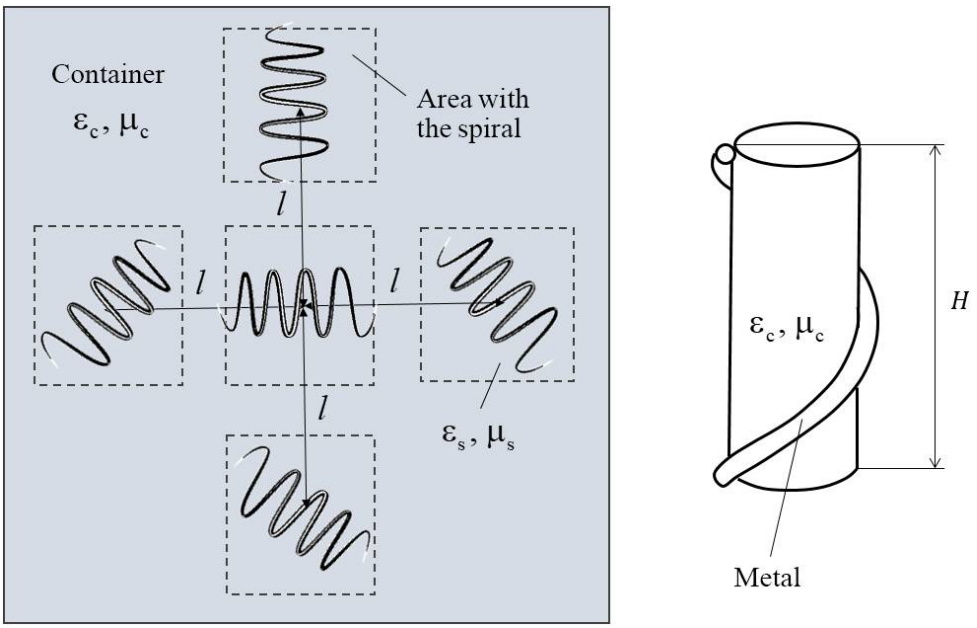

Fig. 2. Cell structure of a chiral metamaterial based on a thin-wire helix
Рис. 2. Структура ячейки кирального метаматериала на основе тонкопроволочной спирали

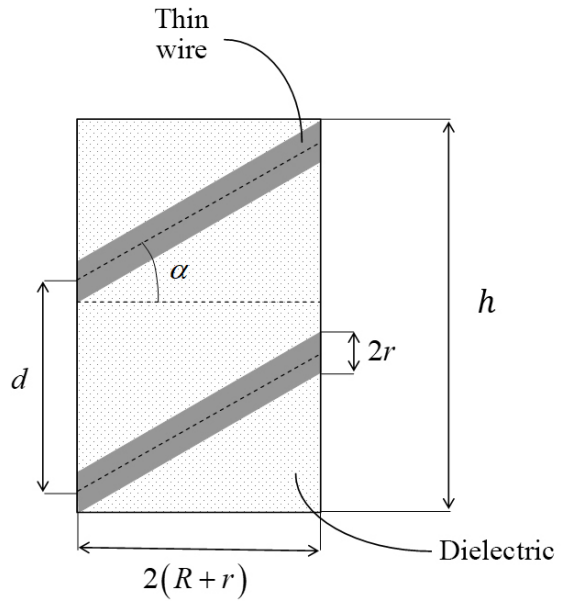

Fig. 3. Cross section of a cylindrical mandrel, on which a thin-wire spiral element is wound
Рис. 3. Поперечный разрез цилиндрической оправки, на которую накручен тонкопроволочный спиральный элемент

The capacitance of the spiral element is determined by the wire capacitance, the interturn capacitance, and the interelement capacitance:

$$C = C_w + C_{it} + C_{ie}. \quad (7)$$

The capacitance of the conductive wire itself is determined using the following equation for the capacitance of a straight conductor:

$$C_w = \varepsilon_c \frac{g}{18\ln\left(\frac{2g}{r}\right) - 1}, \quad (8)$$

where r is the wire radius.

The interturn capacitance of the spiral is determined as follows:

$$C_{it} = \frac{\varepsilon_c S_{it}(N-1)}{d}, \quad (9)$$

where

$$S_{it} = \pi\left[(R+2r)^2 - R^2\right]$$

– area of the ring formed by the wire element; d is the spiral pitch; and N is the number of turns.

The distance between the spiral turns can be expressed in terms of container height h and number of spiral turns N as follows:

$$d = \frac{h}{N+1}, \quad (10)$$

Substituting Eq. (10) into Eq. (9), we obtain:

$$C_{it} = \frac{\varepsilon_c \pi\left[(R+2r)^2 - R^2\right]\left(N^2-1\right)}{h}. \quad (11)$$

The interelement capacitance of the spiral is determined as follows:

$$C_{ie} = \frac{\varepsilon_c S_{ie}}{4l}, \quad (12)$$

where

$$S_{ie} = \frac{4Nr(R+r)}{\cos\alpha}$$

– area of space filled with spirals; r is the wire radius; l is the distance between chiral elements; $\alpha = \pi/\left[2(N+1)\right]$ is spiral winding angle. The coeffi-

cient 1 / 4 is related to the spatial arrangement of the chiral elements in the container.

Substituting the expressions for the twist angle of the helix and the area occupied by the chiral element into Eq. (12), we obtain:

$$C_{ie} = \frac{\varepsilon_c N r (R+r)}{l\cos\left[\frac{\pi}{2(N+1)}\right]}, \quad (13)$$

where R is the inner radius of the spiral; α is spiral winding angle; r is the wire radius; A is the distance between the chiral elements; N is the number of turns; and ε_c is the dielectric permeability of the container.

Substituting Eqs. (9), (11), and (13) into the Eq. (8) representing the total capacity, we obtain:

$$C = \varepsilon_c \frac{g}{18\ln\left(\frac{2g}{r}\right)-1} + \frac{\varepsilon_c r N (R+r)}{l\cos\left[\frac{\pi}{2(N+1)}\right]} + \quad (14)$$

$$+ \frac{\varepsilon_c \pi\left[(R+2r)^2 - R^2\right]\left(N^2-1\right)}{h}.$$

Considering Eqs. (5), (6), and (14) for the resonant frequency of a single-start spiral element, we obtain:

$$\omega_0 = \frac{c\sqrt{g}}{\sqrt{\pi\varepsilon_c\mu_c}NRK_x}; \quad (15)$$

$$K_x = \sqrt{\frac{g}{18\ln\left(\frac{2g}{r}\right)-1} + \frac{\pi\left[(R+2r)^2 - R^2\right]\left(N^2-1\right)}{h} + \frac{rN(R+r)}{l\cos\left[\frac{\pi}{2(N+1)}\right]}}.$$

Eq. (15) was obtained in a quasistatic approximation, and its application is only viable within the range $\omega \in (0;\ \omega_{max})$, where ω_{max} represents the maximum frequency at which the elements can be considered quasistationary $cT \gg 1$ (where c is the speed of light; and T is the period of oscillation of the electromagnetic field).

Thus, a particular mathematical model of a chiral metamaterial, based on a uniform set of thin-wire spiral elements, considers Eqs. (1), (6), and (15) has and takes the following form:

$$\vec{\mathbf{D}} = \varepsilon(\omega)\vec{\mathbf{E}} \mp i\chi(\omega)\vec{\mathbf{H}}, \quad \vec{\mathbf{B}} = \mu\vec{\mathbf{H}} \pm i\chi(\omega)\vec{\mathbf{E}}; \quad (16)$$

$$\varepsilon(\omega) = \varepsilon_c \frac{1+2\alpha\varepsilon_x(\omega)}{1-\alpha\varepsilon_x(\omega)}; \quad \chi(\omega) = \frac{\omega_0^2\beta_0\omega}{\omega_0^2 + 2i\delta_x\omega_0\omega - \omega^2};$$

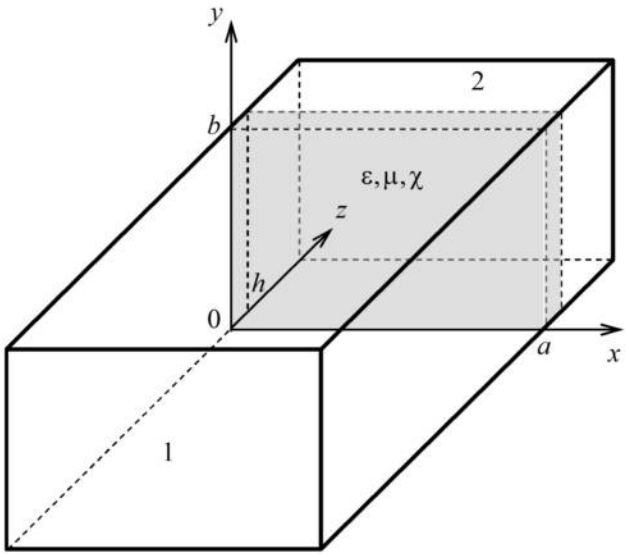

Fig. 4. Geometry of the problem
Рис. 4. Геометрия задачи

$$\varepsilon_x = \frac{\varepsilon_s(\omega)-\varepsilon_c}{\varepsilon_s(\omega)+2\varepsilon_c}; \quad \varepsilon_s(\omega) = \varepsilon_\infty + \frac{(\varepsilon_c-\varepsilon_\infty)\omega_p^2}{\omega_0^2 + 2i\delta_e\omega - \omega^2};$$

$$\omega_0 = \frac{c\sqrt{g}}{\sqrt{\pi\varepsilon_c\mu_c}NRK_x},$$

where

$$K_x = \sqrt{\frac{g}{18\ln\left(\frac{2g}{r}\right)-1} + \frac{\pi\left[(R+2r)^2 - R^2\right]\left(N^2-1\right)}{h} + \frac{rN(R+r)}{l\cos\left[\frac{\pi}{2(N+1)}\right]}}.$$

2. Problem of diffraction of the fundamental wave of a rectangular waveguide H_{10} on a planar transverse insert made of a chiral metamaterial created using thin-wire conducting spiral microelements

This study addresses the issue of H_{10} wave diffraction in a rectangular waveguide on a thin chiral layer, located perpendicular to the power transmission direction. The geometry of the problem is presented in Fig. 4.

At $z = 0$, a thin chiral layer exists with material parameters ε, μ, and χ. The thickness of this chiral layer is less than the wavelength $k_0 h \ll 1$ (where h is the layer thickness; and $k_0 = \omega/c$ is the wave number for a plane homogeneous electromagnetic wave in vacuum). The walls limiting the waveguide at $x = 0; a$

and $y = 0; b$ are assumed to be perfectly conducting ($\sigma = \infty$).

The problem of wave diffraction by a transverse chiral layer in a rectangular waveguide was solved using the method of double-sided boundary conditions (DSBCs) for a thin chiral layer [33].

We assume that a H_{10} wave with components of complex amplitudes of the electromagnetic field E_y, H_x, H_z is incident on the chiral layer from the region $z < 0$. For this geometry, we establish two-sided approximate boundary conditions for a thin chiral layer as follows [33]:

$$E_y^{(1)} - E_y^{(2)} = \frac{\chi h}{2k_0 n_c^2}\frac{\partial^2}{\partial y^2}\left(E_x^{(1)} + E_x^{(2)}\right) + \tag{17}$$

$$+\frac{ik_0 h}{2}\left\{\mu\left(H_x^{(1)} + H_x^{(2)}\right) + i\chi\left(E_x^{(1)} + E_x^{(2)}\right)\right\},$$

$$H_y^{(1)} - H_y^{(2)} = \frac{i\varepsilon' h}{2k_0 n_c^2}\frac{\partial^2}{\partial y^2}\left(E_x^{(1)} + E_x^{(2)}\right) -$$

$$-\frac{ik_0 h}{2}\left\{\varepsilon\left(E_x^{(1)} + E_x^{(2)}\right) - i\chi\left(H_x^{(1)} + H_x^{(2)}\right)\right\},$$

$$E_x^{(1)} - E_x^{(2)} = -\frac{\chi h}{2k_0 n_c^2}\frac{\partial^2}{\partial x^2}\left(E_y^{(1)} + E_y^{(2)}\right) -$$

$$-\frac{ik_0 h}{2}\left\{\mu\left(H_y^{(1)} + H_y^{(2)}\right) + i\chi\left(E_y^{(1)} + E_y^{(2)}\right)\right\},$$

$$H_x^{(1)} - H_x^{(2)} = \frac{i\varepsilon' h}{2k_0 n_c^2}\frac{\partial^2}{\partial x^2}\left(E_y^{(1)} + E_y^{(2)}\right) +$$

$$+\frac{ik_0 h}{2}\left\{\varepsilon\left(E_y^{(1)} + E_y^{(2)}\right) - i\chi\left(H_y^{(1)} + H_y^{(2)}\right)\right\},$$

where $n_c^2(\omega) = \varepsilon(\omega)\mu - \chi^2(\omega)$; the indices "1" and "2" correspond to the areas of the waveguide located at $z < 0$ and $z > h$.

Let us assume that the incident wave H_{10} is incident on the chiral layer from $z = -\infty$ and the waveguide is matched at $z = +\infty$. The field of the incident wave at any inhomogeneity gives rise to the reflection and transmission of the fundamental wave H_{10}. From the solution of the homogeneous Helmholtz equations and considering the boundary conditions at $x = 0; a$ and Maxwell's equations, we formulate equations for the tangential components $E_y^{(j)}$ and $H_x^{(j)}$ ($j = 1, 2$) of the wave field H_{10} in the isotropic regions 1 and 2 [33]:

$$E_y^{(1)} = \left(e^{-i\gamma_{10}z} + R_{10}e^{i\gamma_{10}z}\right)\sin\left(\frac{\pi x}{a}\right); \tag{18}$$

$$E_y^{(2)} = T_{10}e^{-i\gamma_{10}z}\sin\left(\frac{\pi x}{a}\right),$$

$$H_x^{(1)} = -\frac{\gamma_{10}}{k_0}\left(e^{-i\gamma_{10}z} - R_{10}e^{i\gamma_{10}z}\right)\sin\left(\frac{\pi x}{a}\right); \tag{19}$$

$$H_x^{(2)} = -\frac{\gamma_{10}}{k_0}T_{10}e^{-i\gamma_{10}z}\sin\left(\frac{\pi x}{a}\right),$$

where $\gamma_{10} = \sqrt{k_0^2 - \left(\pi/a\right)^2}$ is the wave H_{10} propagation constant in a rectangular waveguide with vacuum filling; and R_{10}, T_{10} are unknown wave H_{10} reflection and transmission coefficients, respectively. The amplitude of the incident wave H_{10} was assumed to be 1.

Owing to the cross-polarization of the field, when wave H_{10} is incident on the chiral layer in regions 1 and 2 of the waveguide, tangential components $E_x^{(j)}$ and $H_y^{(j)}$ ($j = 1, 2$) will also appear, and a cross-polarized wave H_{01} with components will arise (when $a \geq 2b$):

$$E_x^{(1)} = R_{01}e^{i\gamma_{01}z}\sin\left(\frac{\pi y}{b}\right); \tag{20}$$

$$E_x^{(2)} = T_{01}e^{-i\gamma_{01}z}\sin\left(\frac{\pi y}{b}\right);$$

$$H_y^{(1)} = -\frac{\gamma_{01}}{k_0}R_{01}e^{i\gamma_{01}z}\sin\left(\frac{\pi y}{b}\right);$$

$$H_y^{(2)} = \frac{\gamma_{01}}{k_0}T_{01}e^{-i\gamma_{01}z}\sin\left(\frac{\pi y}{b}\right),$$

where $\gamma_{01} = \sqrt{k_0^2 - \left(\pi/b\right)^2}$ is the wave H_{10} propagation constant in a rectangular waveguide with vacuum filling; and R_{01}, T_{01} are the reflection and transmission coefficients of the wave H_{10}, respectively.

Consequently, the equations for the component vectors of the electromagnetic field tangential to the layer have the following form:

$$E_y^{(1)} = \left(e^{-i\gamma_{10}z} + R_{10}e^{i\gamma_{10}z}\right)\sin\left(\frac{\pi x}{a}\right); \tag{21}$$

$$H_y^{(1)} = -\frac{\gamma_{01}}{k_0}R_{01}e^{i\gamma_{01}z}\sin\left(\frac{\pi y}{b}\right);$$

$$E_x^{(1)} = R_{01}e^{i\gamma_{01}z}\sin\left(\frac{\pi y}{b}\right);$$

$$H_x^{(1)} = -\frac{\gamma_{10}}{k_0}\left(e^{-i\gamma_{10}z} - R_{10}e^{i\gamma_{10}z}\right)\sin\left(\frac{\pi x}{a}\right);$$

in region 1;

$$E_y^{(2)} = T_{10}e^{-i\gamma_{10}z}\sin\left(\frac{\pi x}{a}\right); \tag{22}$$

$$H_y^{(2)} = \frac{\gamma_{01}}{k_0}T_{01}e^{-i\gamma_{01}z}\sin\left(\frac{\pi y}{b}\right);$$

$$E_x^{(2)} = T_{01}e^{-i\gamma_{01}z}\sin\left(\frac{\pi y}{b}\right);$$

$$H_x^{(2)} = -\frac{\gamma_{10}}{k_0} T_{10} e^{-i\gamma_{10} z} \sin\left(\frac{\pi x}{a}\right);$$

in region 2.

Substituting Eqs. (21) and (22) into the DSBC of Eq. (17), we obtain a system of four algebraic equations for unknown coefficients R_{10}, R_{01}, T_{10}, T_{01}:

$$\vec{\mathbf{A}}\vec{\mathbf{R}} = \vec{\mathbf{F}}, \quad (23)$$

where $\vec{\mathbf{R}} = \{R_{10}, R_{01}, T_{10}, T_{01}\}$;

$$\vec{\mathbf{F}} = \left\{\left[-1 - \frac{i\mu\gamma_{10}h}{2}\right], \left[\frac{\chi\gamma_{10}h}{2}\right], \left[-\frac{\chi k_0 h}{2}\left(1+\alpha_{10}^2\right)\right], \left[-\frac{\gamma_{10}}{k_0} - \frac{i\varepsilon' k_0 h}{2}\left(1+\alpha_{10}^2\right)\right]\right\}^{\mathrm{T}}.$$

The matrix $\vec{\mathbf{A}}$ elements have the form:

$$A_{11} = 1 - \frac{i\mu\gamma_{10}h}{2}; \quad A_{12} = \frac{\chi k_0 h}{2}\left(1+\alpha_{01}^2\right);$$

$$A_{13} = \left[-1 + \frac{i\mu\gamma_{10}h}{2}\right] e^{-i\gamma_{10}h};$$

$$A_{14} = \frac{\chi k_0 h}{2}\left(1+\alpha_{01}^2\right) e^{-i\gamma_{01}h}; \quad A_{21} = \frac{\chi\gamma_{10}h}{2};$$

$$A_{22} = -\frac{\gamma_{01}}{k_0} + \frac{i\varepsilon k_0 h}{2}\left(1+\alpha_{01}^2\right); \quad A_{23} = -\frac{\chi\gamma_{10}h}{2} e^{-i\gamma_{10}h};$$

$$A_{24} = \left[-\frac{\gamma_{01}}{k_0} + \frac{i\varepsilon k_0 h}{2}\left(1+\alpha_{01}^2\right)\right] e^{-i\gamma_{01}h};$$

$$A_{31} = \frac{\chi k_0 h}{2}\left(1+\alpha_{10}^2\right); \quad A_{32} = \left[-1 + \frac{i\mu\gamma_{01}h}{2}\right];$$

$$A_{33} = \frac{\chi k_0 h}{2}\left(1+\alpha_{10}^2\right) e^{-i\gamma_{10}h};$$

$$A_{34} = \left[1 - \frac{i\mu\gamma_{01}h}{2}\right] e^{-i\gamma_{01}h};$$

$$A_{41} = \left[-\frac{\gamma_{10}}{k_0} + \frac{i\varepsilon k_0 h}{2}\left(1-\alpha_{10}^2\right)\right]; \quad A_{42} = -\frac{\chi\gamma_{01}h}{2};$$

$$A_{43} = \left[-\frac{\gamma_{10}}{k_0} + \frac{i\varepsilon k_0 h}{2}\left(1-\alpha_{10}^2\right)\right] e^{-i\gamma_{10}h};$$

$$A_{44} = \frac{\chi\gamma_{01}h}{2} e^{-i\gamma_{01}h},$$

where $\alpha_{10}^2 = \pi^2/(k_0^2 a^2 n_c^2)$; $\alpha_{01}^2 = \pi^2/(k_0^2 b^2 n_c^2)$. The remaining parameters are determined by the system of equations (16).

Solving the system of equations (23) in the first approximation with respect to the small parameter $k_0 h$, in an analytical form, we derive equations for the reflection and transmission coefficients of the fundamental and cross-polarized waves H_{10} and H_{01}:

$$R_{10} = \frac{k_0 h\varepsilon\left[\frac{\beta_{01}}{\beta_{10}}\right]\left[1+\alpha_{10}+\eta^2\beta_{10}^2\right]}{2i\beta_{10} + k_0 h\varepsilon\left(1+\alpha_{01}\right)\left\{1+\eta^2\beta_{01}^2\left(\beta_{10}-\beta_{01}\right)\right\}}; \quad (24)$$

$$T_{10} = \frac{k_0 h\varepsilon\left(1+\alpha_{01}+\eta^2\beta_{01}^2\right) e^{-ik_0 h\beta_{10}}}{2i\beta_{01} + k_0 h\varepsilon\left(1+\alpha_{01}\right)\left\{1+\eta^2\beta_{01}^2\left(\beta_{10}-\beta_{01}\right)\right\}};$$

$$R_{01} = \frac{i\chi k_0 h\left[-\beta_{10} + \beta_{01}\left(1-\alpha_{10}\right)\right]}{2i\beta_{01} + k_0 h\varepsilon\left(1+\alpha_{01}\right)\left\{1+\eta^2\beta_{01}^2\left(\beta_{10}-\beta_{01}\right)\right\}};$$

$$T_{01} = \frac{i\chi k_0 h\left[\beta_{10} + \beta_{01}\left(1-\alpha_{10}\right)\right] e^{-ik_0 h\beta_{01}}}{2i\beta_{01} + k_0 h\varepsilon\left(1+\alpha_{01}\right)\left\{1+\eta^2\beta_{01}^2\left(\beta_{10}-\beta_{01}\right)\right\}},$$

where

$$\eta = \sqrt{\mu/\varepsilon}; \ \beta_{10} = \sqrt{1-\left[\pi/(k_0 a)\right]^2};$$

$$\beta_{01} = \sqrt{1-\left[\pi/(k_0 b)\right]^2}.$$

3. Numerical modeling

In the numerical modeling, we considered a rectangular waveguide, in which the transverse plane comprised a predetermined thickness layer of chiral metamaterial. The metamaterial container was made of polystyrene foam with a relative dielectric permeability of 1,5. The waveguide was filled with vacuum, which has a relative dielectric permeability of 1. In this study, we calculated the frequency dependencies of the transmitted and reflected powers of the fundamental and cross-polarized waves H_{10} and H_{01} were calculated when the fundamental wave was incident on the chiral layer.

Let us consider the case when the metamaterial is formed by spirals with one twist ($N = 1$).

The initial values of metamaterial parameters are the following:

$\varepsilon_1 = \varepsilon_3 = 1$; $\varepsilon_2 = 1{,}5 - 10^{-5} i$; $N = 1$;
$R = 0{,}0025$ m; $r = 0{,}001$ m;
$d = 0{,}0015$ m; $h = 0{,}005$ m; $l = 0{,}0015$ m.

Figure 5 presents the dependencies of the transmitted $20\lg|T_{10}|$ and reflected $20\lg|R_{10}|$ wave H_{10} powers, as well as the transmitted $20\lg|T_{01}|$ and reflected $20\lg|R_{01}|$ wave H_{01} powers, on frequency in the operating mode of a rectangular waveguide at $N = 1$.

As inferred from Fig. 5, for a CMM based on single-turn spirals, the fundamental wave H_{10} traverses the chiral layer with minimal attenuation. This is because the attenuation of the transmitted power across

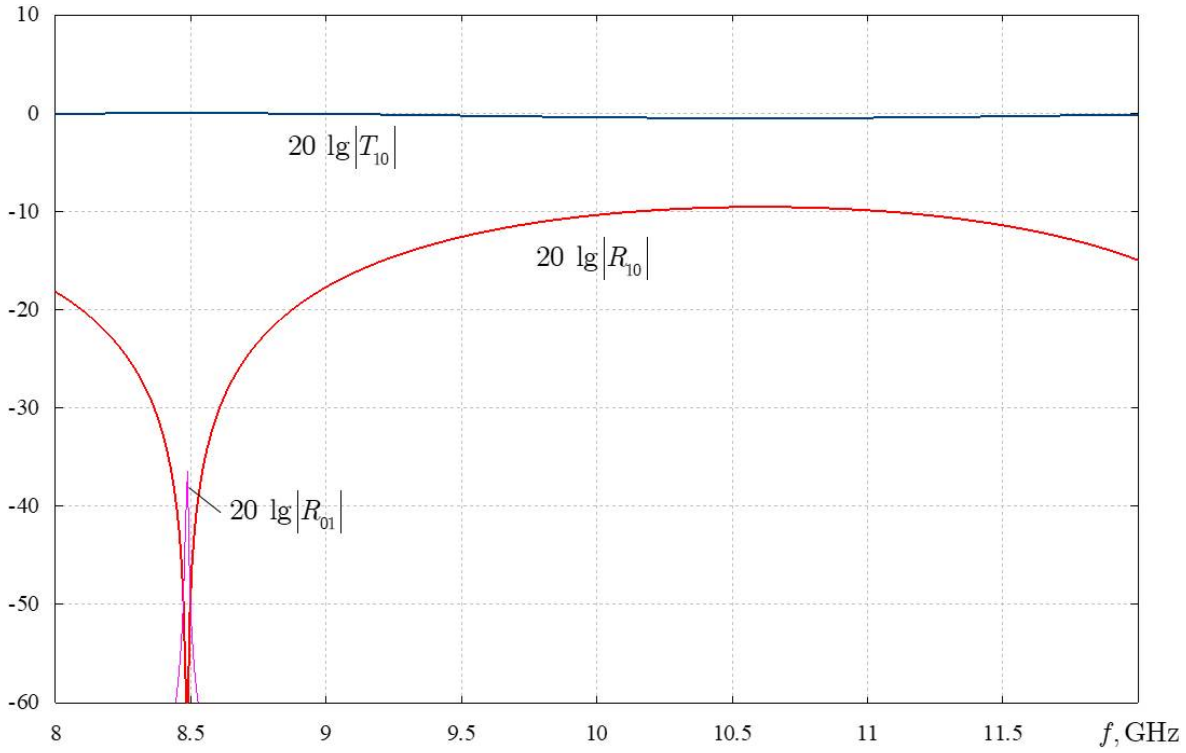

Fig. 5. Frequency dependences of the transmitted and reflected powers for the case of single-turn spirals
Рис. 5. Частотные зависимости прошедшей и отраженной мощностей для случая одновитковых спиралей

all frequencies of the operating range is close to 0 dB. The reflection of the fundamental wave is minimal, reaching a peak at –10 dB around the frequency of 10,5 GHz. There is also a resonant minimum in the reflection of the fundamental wave H_{10} near the frequency of 8,5 GHz. Meanwhile, the cross-polarized wave H_{01} is reflected near the same frequency, but its maximum reflection level is –37,5 dB.

Let us consider the case in which the metamaterial is formed by spirals with two twists $(N = 2)$.

The metamaterial parameter values are the following:

$\varepsilon_1 = \varepsilon_3 = 1; \quad \varepsilon_2 = 1{,}5 - 10^{-5} i; \quad N = 2;$
$R = 0{,}0025$ m; $r = 0{,}001$ m;
$d = 0{,}0015$ m; $h = 0{,}005$ m; $l = 0{,}0015$ m.

Figure 6 presents the dependencies of the transmitted $20\lg|T_{10}|$ and reflected $20\lg|R_{10}|$ wave H_{10} powers, as well as the transmitted $20\lg|T_{01}|$ and reflected $20\lg|R_{01}|$ wave H_{01} powers, on frequency in the operating mode of a rectangular waveguide at $N = 2$.

As is obvious from Fig. 6, with two-turn spirals, frequency selectivity arises. Specifically, at a frequency of 10,9 GHz, there is a sharp dip in the transmission of the fundamental wave through the chiral layer in the waveguide. Near this frequency in a rectangular waveguide, wave H_{01} becomes the fundamental wave because the transmitted and reflected power reaches maxima. The presence of a chiral layer based on two-turn spirals results in the waveguide initially not transmitting the fundamental wave H_{10} near the resonant frequency, and a shift to the operating mode on the cross-polarized wave H_{01}, which becomes the fundamental one, occurs. In addition, Fig. 6 shows both waves over the entire operating frequency range, although the amplitude of the cross-polarized wave is extremely small (except in the region near the resonant frequency).

Let us now consider the case in which the metamaterial is formed by spirals with three twists. The parameter values for the metamaterial are the following:

$\varepsilon_1 = \varepsilon_3 = 1; \quad \varepsilon_2 = 1{,}5 - 10^{-5} i; \quad N = 3;$
$R = 0{,}0025$ m; $r = 0{,}001$ m;
$d = 0{,}0015$ m; $h = 0{,}005$ m; $l = 0{,}0015$ m.

Figure 7 presents the dependencies of the transmitted $20\lg|T_{10}|$ and reflected $20\lg|R_{10}|$ wave H_{10} powers, as well as the transmitted $20\lg|T_{01}|$ and reflected $20\lg|R_{01}|$ wave H_{01} powers, on frequency in the operating mode of a rectangular waveguide at $N = 3$.

As evident from Fig. 7, pronounced frequency selectivity is also present in this case. Near the resonant frequency of 10,1 GHz, the fundamental H_{10} wave ceases to propagate along the waveguide and is partially reflected from the chiral layer, while the cross-

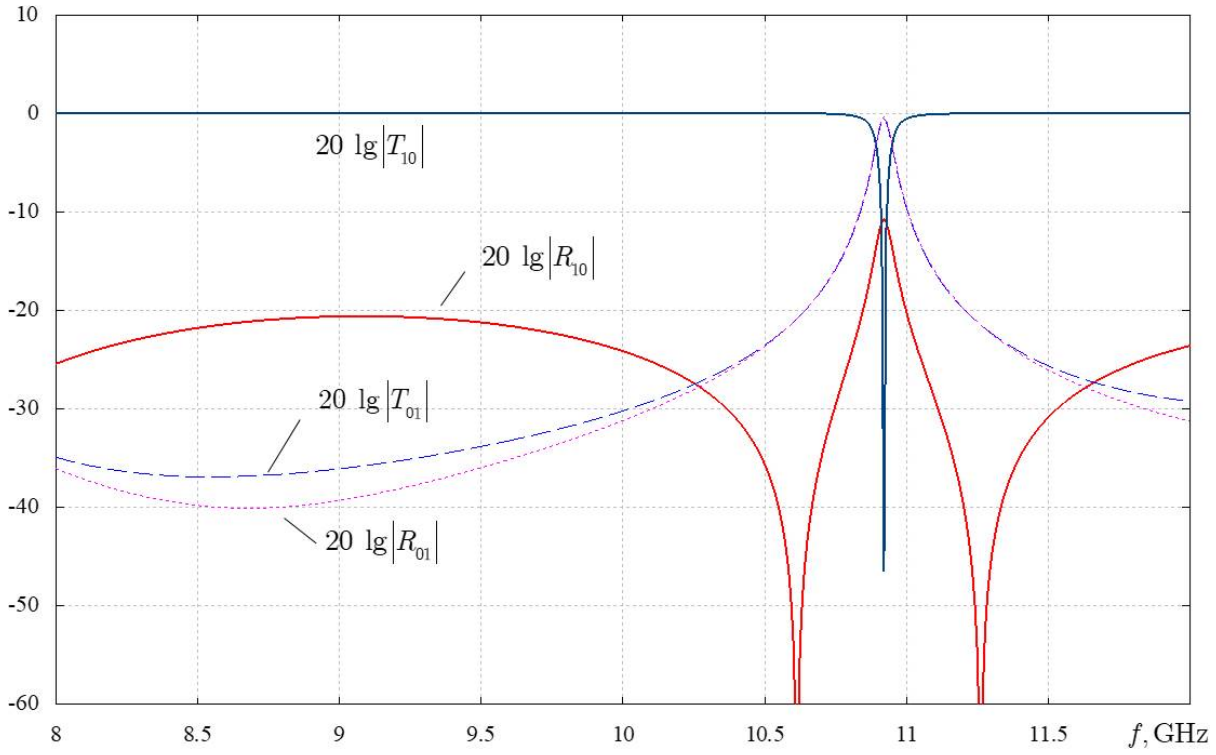

Fig. 6. Frequency dependences of the transmitted and reflected powers for the case of two-turn spirals
Рис. 6. Частотные зависимости прошедшей и отраженной мощностей для случая двухвитковых спиралей

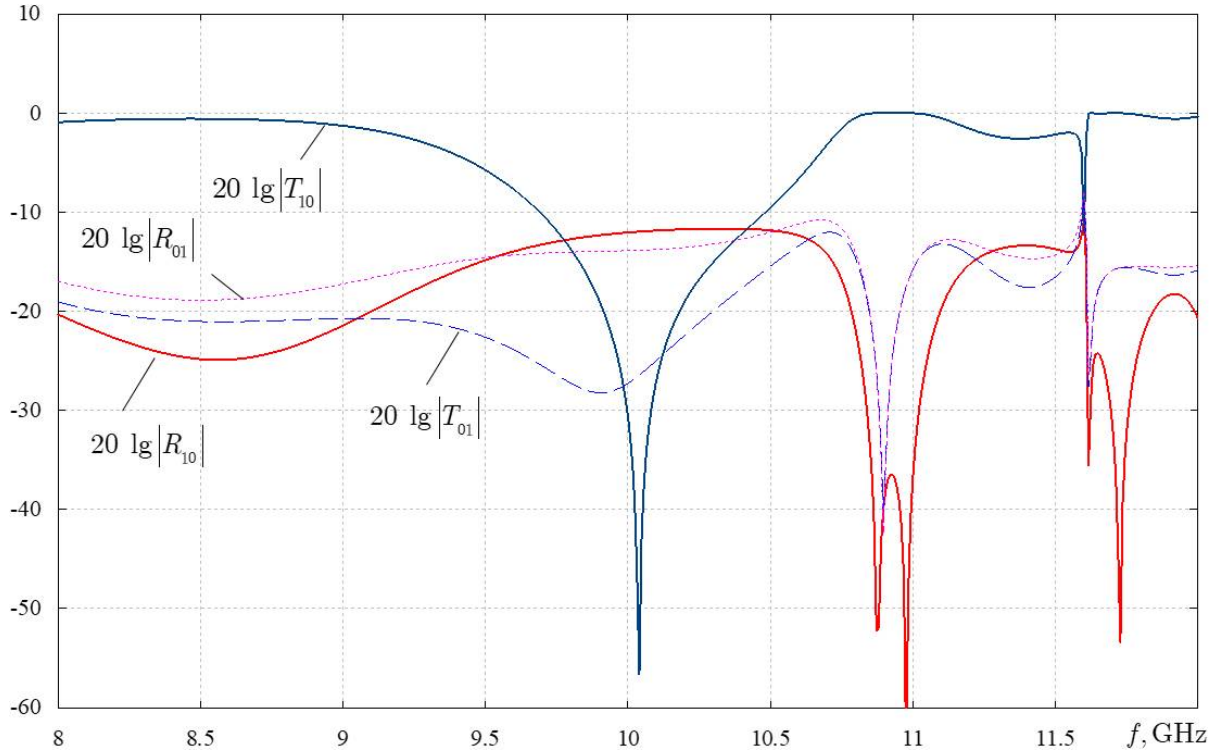

Fig. 7. Frequency dependences of transmitted and reflected powers for the case of three-turn spirals
Рис. 7. Частотные зависимости прошедшей и отраженной мощностей для случая трехвитковых спиралей

polarized wave passes into the region behind the chiral layer with a larger amplitude than that of the fundamental wave. At a frequency of 11,4 GHz, there is a minimum in the transmission of the fundamental wave through the chiral layer in the waveguide. The presence of a chiral layer based on three-turn spirals results in the waveguide initially not transmitting the fundamental wave H_{10} near the resonant frequency, leading to a shift to the operating mode of the cross-polarized wave H_{01}, which becomes the fundamental one.

Throughout our analysis, we conclude that to obtain a strong effect of frequency selectivity, it is preferable to use two- and three-turn spirals as chiral microelements. These enable the mode transition from the fundamental wave type from H_{10} to H_{01} near resonant frequencies. This phenomenon is not associated with waveguide dispersion but arises owing to the insertion of a heterogeneous chiral metamaterial into the waveguide.

Conclusion

This study constructs a mathematical model of achiral metamaterial based on thin-wire conducting spirals, considering the chirality, heterogeneity, and dispersion of material parameters. The work proved the frequency selectivity of wave propagation through a chiral layer located in the transverse plane of a rectangular waveguide. Furthermore, it establishes that a chiral metamaterial based on two-turn thin-wire spirals exhibits the highest degree of frequency selectivity. Our work also revealed that when a chiral metamaterial is inserted into a rectangular waveguide, a cross-polarized wave H_{01} inevitably arises in addition to the wave of the fundamental type H_{10}.

An analysis of the frequency dependencies of the reflection and transmission coefficient modules of the fundamental H_{10} and cross-polarized H_{01} showed that in some narrow frequency intervals in single-wave mode, situations arise when the fundamental wave type transitions from H_{10} to H_{01} near resonant frequencies.

The transmission line under study has potential applications in the creation of frequency-selective filters and polarization converters in the microwave range.

References

1. Capolino F. *Theory and Phenomena of Metamaterials*. Boca Raton: Taylor & Francis – CRC Press, 2009, 992 p.
2. Engheta N., Ziolkowski R.W. *Metamaterials: Physics and Engineering Explorations*. Hoboken: Wiley, 2006, 414 p.
3. Iyer A.K., Alù A., Epstein A. Metamaterials and metasurfaces – historical context, recent advances, and future directions. *IEEE Transactions on Antennas and Propagation*, 2020, vol. 68, no. 3, pp. 1223–1231. DOI: https://doi.org/10.1109/TAP.2020.2969732
4. Pendry J. A chiral route to negative refraction. *Science*, 2004, vol. 306, no. 5700, pp. 1353–1355. DOI: https://doi.org/10.1126/science.1104467
5. Zheludev N.I. A Roadmap for metamaterials. *Opt. Photonics News*, 2011, vol. 22, no. 3, pp. 30–35. DOI: https://doi.org/10.1364/OPN.22.3.000030
6. Lindell I.V. et al. *Electromagnetic Waves in Chiral and Bi-Isotropic Media*. London: Artech House, 1994, 291 p.
7. Lakhtakia A., Varadan V.K., Varadan V.V. *Time-Harmonic Electromagnetic Fields in Chiral Media. Lecture Notes in Physics*. Berlin: Springer-Verlag, 1989, 121 p.
8. Caloz C., Sihvola A. Electromagnetic chirality, Part 1: The microscopic perspective [electromagnetic perspectives]. *IEEE Antennas and Propagation Magazine*, 2020, vol. 62, no. 1, pp. 58–71. DOI: https://doi.org/10.1109/MAP.2019.2955698
9. Tret'yakov S.A. Electrodynamics of complex media: chiral, bi-isotropic and some bianisotropic materials. *Radiotekhnika i elektronika*, 1994, vol. 39, no. 10, pp. 1457–1470. (In Russ.)
10. Katsenelenbaum B.Z. et al. Chiral electrodynamic objects. *Uspekhi fizicheskikh nauk*, 1997, vol. 167, no. 11, pp. 1201–1212. DOI: https://doi.org/10.3367/UFNr.0167.199711c.1201 (In Russ.)
11. Slyusar V.I. Metamaterials in antenna technology: history and basic principles. *Elektronika: NTB*, 2009, no. 7, pp. 10–19. URL: https://www.electronics.ru/files/article_pdf/0/article_287_909.pdf (In Russ.)
12. Vendik I.B., Vendik O.G. Metamaterials and their application in microwave technology (Review). *Zhurnal tekhnicheskoy fiziki*, 2013, vol. 83, no. 1, pp. 3–28. URL: https://journals.ioffe.ru/articles/viewPDF/41403 (In Russ.)
13. Pozar D.M. Microstrip antennas and arrays on chiral substrates. *IEEE Transactions on Antennas and Propagation*, 1992, vol. 40, no. 10, pp. 1260–1263. DOI: https://doi.org/10.1109/8.182462
14. Varadan V.K., Varadan V.V., Lakhtakia A. Propagation in parallel-plate wave-guide wholly filled with a chiral medium. *Journal of Wave-Material Interaction*, 1988, vol. 3, no. 3, pp. 267–272.
15. Cory H., Rosenhouse I. Electromagnetic wave propagation along a chiral slab. *IEE Proceedings H (Microwaves, Antennas and Propagation)*, 1991, vol. 138, no. 1, pp. 51–54. DOI: https://doi.org/10.1049/ip-h-2.1991.0009
16. Oksanen M.I., Koivisto P., Tretyakov S.A. Vector circuit method applied for chiral slab waveguides. *Journal of Lightwave Technology*, 1992, vol. 10, no. 2, pp. 150–155. DOI: https://doi.org/10.1109/50.120569

17. Eftimiu C., Pearson L.W. Guided electromagnetic waves in chiral media. *Radio Science*, 1989, vol. 24, no. 3, pp. 351–359. DOI: https://doi.org/10.1029/RS024i003p00351

18. Neganov V.A., Osipov O.V. Eigenwaves of a plane two-layer chiral-dielectric waveguide. *Radiotekhnika*, 2003, no. 5, pp. 21–25. (In Russ.)

19. Pelet P., Engheta N. The theory of chirowaveguides. *IEEE Transactions on Antennas and Propagation*, 1990, vol. 38, no. 1, pp. 90–98. DOI: https://doi.org/10.1109/8.43593

20. Oksanen M.I., Koivisto P.K., Tretyakov S.A. Plane chiral waveguides with boundary impedance conditions. *Microwave and Optical Technology Letters*, 1992, vol. 5, no. 2, pp. 68–72. DOI: https://doi.org/10.1002/mop.4650050207

21. Pelet P., Engheta N. Modal analysis for rectangular chirowaveguides with metallic walls using the finite-difference method. *Journal Electromagnetic Waves and Applications*, 1992, vol. 6, no. 9, pp. 1277–1285. DOI: https://doi.org/10.1163/156939392X00724

22. Moiseeva N.M. Eigen modes of planar chiral waveguides. *Computer Optics*, 2014, vol. 38, no. 2, pp. 198–203. DOI: https://doi.org/10.18287/0134-2452-2014-38-2-198-203

23. Kamenetskii E.O. On the technology of making chiral and bianisotropic waveguides for microwave propagation. *Microwave and Optical Technology Letters*, 1996, vol. 11, no. 2, pp. 103–107. DOI: https://doi.org/10.1002/(SICI)1098-2760(19960205)11:2%3C103::AID-MOP17%3E3.0.CO;2-F

24. Aralkin M.V., Dement'ev A.N., Osipov O.V. Mathematical models of chiral metamaterials based on multi-pass conducting elements. *Physics of Wave Processes and Radio Systems*, 2020, vol. 23, no. 1, pp. 8–19. DOI: https://doi.org/10.18469/1810-3189.2020.23.1.8-19 (In Russ.)

25. Aralkin M.V., Dement'ev A.N., Osipov O.V. Investigation of the electromagnetic characteristics of planar chiral metastructures based on compound helical components, taking into account the heterogeneous Bruggeman model. *Physics of Wave Processes and Radio Systems*, 2020, vol. 23, no. 3, pp. 44–55. DOI: https://doi.org/10.18469/1810-3189.2020.23.3.44-55 (In Russ.)

26. Neshcheret A.M. Development of theoretical foundations and methods for studying radiating and reradiating structures based on chiral metamaterials: dis. ... d-ra. fiz.-mat. nauk. Samara, 2012, 379 p.

27. Sushko M.Ya., Kris'kiv S.K. Compact group method in the theory of permittivity of heterogeneous systems. *Zhurnal tekhnicheskoy fiziki*, 2009, vol. 79, no. 3, pp. 97–101. URL: https://journals.ioffe.ru/articles/9645 (In Russ.)

28. Bruggeman D.A.G. Berechnung verschiedener physikalischer Konstanten von eterogenen Substanzen, I. Dielektrizitatskonstanten und Leitfahigkeiten der Mischkorper aus isotropen Substanzen. *Ann. Phys*., 1935, vol. 416, no. 7, pp. 636–664. DOI: https://doi.org/10.1002/andp.19354160705

29. Garnett J.C. Maxwell. Colours in metal glasses and in metallic films. *Phylos. Trans. R. Soc. London. Ser. A*, 1904, vol. 203, pp. 385–420.

30. Semchenko I.V., Tretyakov S.A., Serdyukov A.N. Research on chiral and bianisotropic media in Byelorussia and Russia in the last ten years. *Progress in Electromagnetics Research*, 1996, vol. 12, pp. 335–370.

31. Condon E.U. Theories of optical rotatory power. *Rev. Mod. Phys.*, 1937, vol. 9, no. 4, pp. 432–457. DOI: https://doi.org/10.1103/RevModPhys.9.432

32. Osipov O.V., Yurasov V.I., Pocheptsov A.O. Chiral metamaterial for frequency selective energy concentration of microwave radiation. *Infokommunikacionnye tehnologii*, 2014, vol. 12, no. 4, pp. 76–82. (In Russ.)

33. Neganov V.A., Osipov O.V. *Reflective, Waveguide and Radiating Structures with Chiral Elements*. Moscow: Radio i svyaz', 2006, 280 p. (In Russ.)

34. Bespalov A.N. et al. Study of antenna complexes using chiral metamaterials and fractal geometry of emitters for MIMO systems. *Physics of Wave Processes and Radio Systems*, 2020, vol. 23, no. 4, pp. 97–110. DOI: https://doi.org/10.18469/1810-3189.2020.23.4.97-110 (In Russ.)

35. Neganov V.A., Gradinar' I.M. Electrodynamic properties of ordered metamaterials. *Physics of Wave Processes and Radio Systems*, 2012, vol. 15, no. 1, pp. 18–24. (In Russ.)

Список литературы

1. Capolino F. Theory and Phenomena of Metamaterials. Boca Raton: Taylor & Francis – CRC Press, 2009. 992 p.

2. Engheta N., Ziolkowski R.W. Metamaterials: Physics and Engineering Explorations. Hoboken: Wiley, 2006. 414 p.

3. Iyer A.K., Alù A., Epstein A. Metamaterials and Metasurfaces – Historical Context, Recent Advances, and Future Directions // IEEE Transactions on Antennas and Propagation, 2020. Vol. 68, no. 3. P. 1223–1231. DOI: https://doi.org/10.1109/TAP.2020.2969732

4. Pendry J. A chiral route to negative refraction // Science. 2004. Vol. 306, no. 5700. P. 1353–1355. DOI: https://doi.org/10.1126/science.1104467

5. Zheludev N.I. A Roadmap for metamaterials // Opt. Photonics News. 2011. Vol. 22, no. 3. P. 30–35. DOI: https://doi.org/10.1364/OPN.22.3.000030

6. Electromagnetic Waves in Chiral and Bi-Isotropic Media / I.V. Lindell [et al.]. London: Artech House, 1994. 291 p.

7. Lakhtakia A., Varadan V.K., Varadan V.V. Time-Harmonic Electromagnetic Fields in Chiral Media. Lecture Notes in Physics. Berlin: Springer-Verlag, 1989. 121 p.

8. Caloz C., Sihvola A. Electromagnetic chirality, Part 1: The microscopic perspective [electromagnetic perspectives] // IEEE Antennas and Propagation Magazine. 2020. Vol. 62, no. 1. P. 58–71. DOI: https://doi.org/10.1109/MAP.2019.2955698

9. Третьяков С.А. Электродинамика сложных сред: киральные, би-изотропные и некоторые бианизотропные материалы // Радиотехника и электроника. 1994. Т. 39, № 10. С. 1457–1470.

10. Киральные электродинамические объекты / Б.З. Каценеленбаум [и др.] // Успехи физических наук. 1997. Т. 167, № 11. С. 1201–1212. DOI: https://doi.org/10.3367/UFNr.0167.199711c.1201

11. Слюсар В.И. Метаматериалы в антенной технике: история и основные принципы // Электроника: НТБ. 2009. № 7. С. 10–19. URL: https://www.electronics.ru/files/article_pdf/0/article_287_909.pdf

12. Вендик И.Б., Вендик О.Г. Метаматериалы и их применение в технике сверхвысоких частот (Обзор) // Журнал технической физики. 2013. Т. 83, № 1. С. 3–28. URL: https://journals.ioffe.ru/articles/viewPDF/41403

13. Pozar D.M. Microstrip antennas and arrays on chiral substrates // IEEE Transactions on Antennas and Propagation. 1992. Vol. 40, no. 10. P. 1260–1263. DOI: https://doi.org/10.1109/8.182462

14. Varadan V.K., Varadan V.V., Lakhtakia A. Propagation in parallel-plate wave-guide wholly filled with a chiral medium // Journal of Wave-Material Interaction. 1988. Vol. 3, no. 3. P. 267–272.

15. Cory H., Rosenhouse I. Electromagnetic wave propagation along a chiral slab // IEE Proceedings H (Microwaves, Antennas and Propagation). 1991. Vol. 138, no. 1. P. 51–54. DOI: https://doi.org/10.1049/ip-h-2.1991.0009

16. Oksanen M.I., Koivisto P., Tretyakov S.A. Vector circuit method applied for chiral slab waveguides // Journal of Lightwave Technology. 1992. Vol. 10, no. 2. P. 150–155. DOI: https://doi.org/10.1109/50.120569

17. Eftimiu C., Pearson L.W. Guided electromagnetic waves in chiral media // Radio Science. 1989. Vol. 24, no. 3. P. 351–359. DOI: https://doi.org/10.1029/RS024i003p00351

18. Неганов В.А., Осипов О.В. Собственные волны плоского двухслойного кирально-диэлектрического волновода // Радиотехника. 2003. № 5. С. 21–25.

19. Pelet P., Engheta N. The theory of chirowaveguides // IEEE Transactions on Antennas and Propagation. 1990. Vol. 38, no. 1. P. 90–98. DOI: https://doi.org/10.1109/8.43593

20. Oksanen M.I., Koivisto P.K., Tretyakov S.A. Plane chiral waveguides with boundary impedance conditions // Microwave and Optical Technology Letters. 1992. Vol. 5, no. 2. P. 68–72. DOI: https://doi.org/10.1002/mop.4650050207

21. Pelet P., Engheta N. Modal analysis for rectangular chirowaveguides with metallic walls using the finite-difference method // Journal Electromagnetic Waves and Applications. 1992. Vol. 6, no. 9. P. 1277–1285. DOI: https://doi.org/10.1163/156939392X00724

22. Moiseeva N.M. Eigen modes of planar chiral waveguides // Computer Optics. 2014. Vol. 38, no. 2. P. 198–203. DOI: https://doi.org/10.18287/0134-2452-2014-38-2-198-203

23. Kamenetskii E.O. On the technology of making chiral and bianisotropic waveguides for microwave propagation // Microwave and Optical Technology Letters. 1996. Vol. 11, no. 2. P. 103–107. DOI: https://doi.org/10.1002/(SICI)1098-2760(19960205)11:2%3C103::AID-MOP17%3E3.0.CO;2-F

24. Аралкин М.В., Дементьев А.Н., Осипов О.В. Математические модели киральных метаматериалов на основе многозаходных проводящих элементов // Физика волновых процессов и радиотехнические системы. 2020. Т. 23, № 1. С. 8–19. DOI: https://doi.org/10.18469/1810-3189.2020.23.1.8-19

25. Аралкин М.В., Дементьев А.Н., Осипов О.В. Исследование электромагнитных характеристик планарных киральных метаструктур на основе составных спиральных компонентов с учетом гетерогенной модели Бруггемана // Физика волновых процессов и радиотехнические системы, 2020. Т. 23, № 3. С. 44–55. DOI: https://doi.org/10.18469/1810-3189.2020.23.3.44-55

26. Нещерет А.М. Разработка теоретических основ и методов исследований излучающих и переизлучающих структур на основе киральных метаматериалов: дис. ... д-ра. физ.-мат. наук. Самара, 2012. 379 с.

27. Сушко М.Я., Криськив С.К. Метод компактных групп в теории диэлектрической проницаемости гетерогенных систем // Журнал технической физики. 2009. Т. 79, № 3. С. 97–101. URL: https://journals.ioffe.ru/articles/9645

28. Bruggeman D.A.G. Berechnung verschiedener physikalischer Konstanten von eterogenen Substanzen, I. Dielektrizitatskonstanten und Leitfahigkeiten der Mischkorper aus isotropen Substanzen // Ann. Phys. 1935. Vol. 416, no. 7. P. 636–664. DOI: https://doi.org/10.1002/andp.19354160705

29. Garnett J.C. Maxwell. Colours in metal glasses and in metallic films // Phylos. Trans. R. Soc. London. Ser. A. 1904. Vol. 203. P. 385–420.

30. Semchenko I.V., Tretyakov S.A., Serdyukov A.N. Research on chiral and bianisotropic media in Byelorussia and Russia in the last ten years // Progress in Electromagnetics Research. 1996. Vol. 12. P. 335–370.

31. Condon E.U. Theories of optical rotatory power // Rev. Mod. Phys. 1937. Vol. 9, no. 4. P. 432–457. DOI: https://doi.org/10.1103/RevModPhys.9.432

32. Осипов О.В., Юрасов В.И., Почепцов А.О. Киральный метаматериал для частотно-селективной концентрации энергии сверхвысокочастотного излучения // Инфокоммуникационные технологии. 2014. Т. 12, № 4. С. 76–82.

33. Неганов В.А., Осипов О.В. Отражающие, волноведущие и излучающие структуры с киральными элементами. М.: Радио и связь, 2006. 280 с.

34. Исследование антенных комплексов с использованием киральных метаматериалов и фрактальной геометрии излучателей для систем MIMO / А.Н. Беспалов [и др.] // Физика волновых процессов и радиотехнические системы. 2020. Т. 23, № 4. С. 97–110. DOI: https://doi.org/10.18469/1810-3189.2020.23.4.97-110

35. Неганов В.А., Градинарь И.М. Электродинамические свойства упорядоченных метаматериалов // Физика волновых процессов и радиотехнические системы. 2012. Т. 15, № 1. С. 18–24.

Физика волновых процессов и радиотехнические системы
2023. Т. 26, № 1. С. 93–105

DOI 10.18469/1810-3189.2023.26.1.93-105
УДК 537.876.46

Дата поступления 6 декабря 2022
Дата принятия 9 января 2023

Исследование электромагнитных свойств поперечной вставки на основе планарного слоя кирального метаматериала в прямоугольном волноводе

И.Ю. Бучнев, О.В. Осипов

Поволжский государственный университет телекоммуникаций и информатики
443010, Россия, г. Самара,
ул. Л. Толстого, 23

Аннотация – В работе рассмотрено решение задачи дифракции основной волны прямоугольного волновода H_{10} на планарной поперечной вставке из кирального метаматериала, созданного на основе тонкопроволочных проводящих спиральных микроэлементов. Для описания кирального слоя построена частная математическая модель, учитывающая свойства гетерогенности и дисперсии диэлектрической проницаемости и параметра киральности искусственной среды. Для учета свойства гетерогенности использовалась известная в физике модель Максвелла Гарнетта. Для учета дисперсии диэлектрической проницаемости была применена формула Друде – Лоренца, а для параметра киральности – формула Кондона. Решение задачи дифракции основной волны прямоугольного волновода на планарном слое из кирального метаматериала проводилось методом частичных областей и было сведено к системе линейных алгебраических уравнений относительно неизвестных коэффициентов отражения и прохождения. Показано, что при наличии поперечного кирального слоя в волноведущей структуре возникает кросс-поляризованная по отношению к основной волна типа H_{01}. Анализ частотных зависимостей модулей коэффициентов отражения и прохождения основной H_{10} и кросс-поляризованной H_{01} показал, что в некоторых узких интервалах частот в одноволновом режиме возникают ситуации, когда реализуется режим замены основного типа волны с H_{10} на H_{01} вблизи резонансных частот. Рассматриваемая линия передачи может найти применение при создании частотно-селективных фильтров и преобразователей поляризации СВЧ-диапазона.

Ключевые слова – киральная среда; киральный метаматериал; метаматериал; спираль; пространственная дисперсия; частотная селективность; модель Максвелла Гарнетта; модель Кондона; прямоугольный волновод; одноволновый режим; основная волна; кросс-поляризация.

Information about the Authors

Ivan Yu. Buchnev, born in 1995, post-graduate student of the Department of Higher Mathematics, Povolzhskiy State University of Telecommunications and Informatics, Samara, Russia.
Research interests: electrodynamics of metamaterials.
E-mail: v.buchnev@psuti.ru

Oleg V. Osipov, born in 1975, Doctor of Physical and Mathematical Sciences, acting head of the Department of Higher Mathematics, Povolzhskiy State University of Telecommunications and Informatics, Samara, Russia.
Research interests: electrodynamics of metamaterials, microwave devices and antennas, nonlinear optics.
E-mail: o.osipov@psuti.ru

Информация об авторах

Бучнев Иван Юрьевич, 1995 г. р., аспирант кафедры высшей математики Поволжского государственного университета телекоммуникаций и информатики, г. Самара, Россия.
Область научных интересов: электродинамика метаматериалов.
E-mail: v.buchnev@psuti.ru

Осипов Олег Владимирович, 1975 г. р., доктор физико-математических наук, и.о. заведующего кафедрой высшей математики Поволжского государственного университета телекоммуникаций и информатики, г. Самара, Россия.
Область научных интересов: электродинамика метаматериалов, устройства СВЧ и антенны, нелинейная оптика.
E-mail: o.osipov@psuti.ru